J. Fluid Mech. (1991), *vol.* 230, *pp.* 339–353
Printed in Great Britain

Numerical simulations of the quasi-stationary stage of ripple excitation by steep gravity–capillary waves

By K. D. RUVINSKY,† F. I. FELDSTEIN AND G. I. FREIDMAN

Institute of Applied Physics, Academy of Sciences of the USSR, 46 Uljonov Street, 603600, Gorky, USSR

(Received 24 January 1990 and in revised form 25 February 1991)

The dependence of the parameters of capillary–gravity ripples on the characteristics of the steep surface waves (in the range 4–20 cm) that excite them is found. For steep 4–6 cm waves calculations are performed on the basis of the improved first Stokes method. Qualitative coincidence of the theoretical results with the experimental data is shown. For 7–20 cm waves the results are obtained by the multiple-scale method where the large-scale motion and the driving force for the ripple are found by the improved first Stokes method. Qualitative agreement between theory and experiment in this wavelength range is achieved.

1. Introduction

A typical effect observed during propagation of steep surface waves (with length from at least 20–25 cm) is the excitation of ripples on wave crests with a characteristic length of several millimetres. This phenomenon was theoretically investigated by Longuet-Higgins (1963) on the basis of the multiple-scale method. As the zeroth approximation Longuet-Higgins (1963) used strongly nonlinear symmetrical gravity waves found as by Davis (1951). Longuet-Higgins (1963) considered the ripples to be linear and purely capillary, and explained the increase of their amplitude by a sharpening of the crests of steep waves. This theory was generalized by Crapper (1970) for the case of nonlinear capillary ripples. The necessity of taking the capillary–gravity nature of the ripples into consideration was shown by Ruvinsky & Freidman (1981). It leads to the possibility of the appearance of group synchronism of ripples and steep waves (which in principle cannot be reached for capillary ripples). It changes the nature of the dependence of the ripple characteristics on the steep wave parameters, as well as affecting the nonlinear damping of these waves caused by ripple excitation.

To test the existing theoretical concepts, Chang, Wagner & Henry (1978) and Ermakov *et al.* (1986) did laboratory investigations of the ripple excitation phenomenon. The results of Chang *et al.* (1978) showed considerable asymmetry of the steep wave shapes and also the character of the changing ripple frequency and amplitude along the wave profiles. Ermakov *et al.* (1986) measured the dependence of the steepness, wavelengths and frequencies of the capillary–gravity ripples (CGR) on the amplitudes and frequencies of the steep waves; they tested the stationarity of CGR excitation, and measured the nonlinear damping of long waves. The experiment of Ermakov *et al.* (1986) showed that the phase synchronism of CGR and steep waves assumed in theoretical papers available at that time (Longuet-Higgins

† Present address: 37/6 Yosef Street, Hadar, Haifa 33145, Israel.

1963 and its generalization by Ruvinsky & Freidman 1981) is well justified and that steep wave attenuation is caused mainly by ripple excitation. Nevertheless, the experiments of Ermakov *et al.* (1986) and the approximate theory which had been developed up to that time, yield an essentially different relationship between ripple parameters and steep wave characteristics. The theory predicted that ripple excitation must begin with large steepness of strong waves (about the steepness where they would start to break if capillarity were disregarded), and an increase of ripple steepness is accompanied by an increase of its wavelength and is determined by approach to group synchronism of ripples and a steep wave (Ruvinsky & Freidman 1981). On the other hand, the experiment shows (Ermakov *et al.* 1986) that ripple excitation begins with strong wave steepness 4–5 times less than the limiting one (i.e. gravity–capillary waves (GCW) become strongly nonlinear with relatively small steepness) and as the ripple steepness increases its wavelength remains practically constant. Thus, the experiments of Ermakov *et al.* (1986) showed the necessity of creating a more detailed theory of ripple excitation.

Recently much progress has been made in the numerical description of stationary GCW of finite amplitude (Rottman & Olfe 1979; Schwartz & Vanden-Broeck 1979; Chen & Saffman 1979, 1980; Hogan 1980, 1981) and in the investigation of their stability (see e.g. Saffman & Yuen 1985; Zhang & Melville 1987). Nevertheless, a description of the ripple excitation phenomenon based on these methods has not been adequately achieved, since it is not clear how to take dissipation of ripples and GKW into consideration.

Ruvinsky & Freidman (1985*a*, *b*, 1987) suggested that ripple excitation by steep GCW should be investigated using the boundary conditions for the potential component of the flow, where the influence of viscosity could be taken into account by approximation or simulation (the quasi-potential approximation), and using a method of solving the equations that can be called the improved first Stokes method. Early results on the numerical simulation of ripple excitation were reported by Ruvinsky & Freidman (1985*b*, 1987).

In this paper the improved first Stokes method is generalized (compared to Ruvinsky & Freidman (1985*b*, 1987, where only the GCW harmonic amplitude damping is taken into account) to the case of time-dependent phases of the harmonics. Detailed calculations of the excited CGR characteristics in the quasi-potential approximation on the basis of this method are given. Good agreement of the numerical results with the experimental data of Ermakov *et al.* (1986) is shown. The upper limit on wavelength ($\Lambda = 6$ cm) and steepness of GCW for which the results can be obtained by this method is determined by the limited capabilities of the computers in use. It is shown that, for longer GCW, results which are in qualitative agreement with the experiment can be obtained using the multiple-scale method where the lower harmonics (they all form a large-scale flow) and the driving force for small-scale motion (a ripple) can be found by the improved first Stokes method. This is achieved by taking into account the influence of surface tension on GCW as well as the finite nature of the ripple source region and the inhomogeneity of fluid velocity in GCW in this region (neglect of these factors by Longuet-Higgins (1963) and Ruvinsky & Freidman (1981) leads to a qualitative disagreement between their theoretical results and the experimental results of Ermakov *et al.* (1986)).

2. Generalization of Stokes method

It is well known that when describing the CGR excitation phenomenon the dissipative processes must be taken into account. In an exact formulation, this problem has not yet been solved, even with a computer. A simplification is possible, however, at a low viscosity. Ruvinsky & Freidman (1985*a*, *b*, 1987) showed (see also the Appendix) that in this case it is possible to express the vortex component of fluid velocity through the potential component and consider the problem in the quasi-potential approximation:

$$\nabla^2\phi = 0, \tag{1a}$$

$$\left.\begin{aligned} \alpha\frac{\partial\phi}{\partial t}+\tfrac{1}{2}\epsilon\alpha(\nabla\phi)^2+\eta-\frac{T\eta_{xx}}{[1+\epsilon^2\eta_x^2]^{\frac{3}{2}}}+2\nu_1\frac{\partial^2\phi}{\partial z^2} &= 0, && (1b)\\ \frac{\partial\eta}{\partial t}+\epsilon\frac{\partial\eta}{\partial x}\frac{\partial\phi}{\partial x} &= \frac{\partial\phi}{\partial z}+v_z, && (1c) \end{aligned}\right\} \quad z=\epsilon\eta,$$

$$\frac{\partial\phi}{\partial z}\to 0 \quad \text{at} \quad z\to-\infty. \tag{1d}$$

System (1) is in dimensionless form. Here $\epsilon\phi = (k/c)\,\phi_1$ is the potential; $\epsilon\eta = k\eta_1$, the surface displacement; $\epsilon v_z = v_{1z_1}/c$, the vertical component of the vortex part of fluid velocity, which can be found from

$$\alpha\frac{\partial v_z}{\partial t} = 2\nu_1\frac{\partial^3\phi}{\partial x^2\,\partial z}\bigg|_{z=\epsilon\eta}. \tag{1e}$$

Here $\alpha = (c/c_0)^2$, $c_0 = (gk)^{\frac{1}{2}}$, c is the phase velocity of GCW; $k = 2\pi/\Lambda$, the wavenumber; ϵ a small parameter. The dimensionless coefficients $T = \gamma k/c_0^2$ and $\nu_1 = \nu kc/c_0^2$ characterize the influence of surface tension and viscosity; $x = kx_1$, $y = ky_1$ are the Cartesian coordinates, and $t = kct_1$.

In the case of the space-periodic GCW that we are interested in, the quantities ϕ and η are periodic functions of the phase $\xi = x-t$, the amplitudes of which change with time as $\exp(-\int_0^t \delta_1\,\mathrm{d}t)$, $\delta_1 = \delta^*/kc$. Since ϕ satisfies the Laplace equation, it can be represented as a sum of Fourier harmonics with amplitudes slowly varying with time and exponentially dependent on the vertical coordinate z, as well as on the t linear term

$$\phi = \phi_0 t+\exp\left[-\int_0^t\delta_1\,\mathrm{d}t\right]\sum_{n=1}^{N}\left(A_n\exp\left[-\int_0^t(\delta_n-\delta_1)\,\mathrm{d}t\right]\sin n\xi \right.$$
$$\left. +B_n\exp\left[-\int_0^t(\beta_n-\delta_1)\,\mathrm{d}t\right]\cos n\xi\right)\mathrm{e}^{nz}, \tag{2}$$

where $A_1 = 1, B_1 = 0$.

Ruvinsky & Freidman (1985*a*, *b*, 1987) noted that with this form of the potential it is possible to integrate the kinematic boundary condition (1*c*) and express the unknown surface η through the potential harmonics. Defining v_z from (1*e*) we can write this integral in the form

$$\eta(\xi,t) = \eta_0(\eta,\xi,t)+\delta_1\left[\frac{1}{\delta_1}\int_0^\xi\frac{\partial\eta}{\partial t}\mathrm{d}\xi-\frac{\bar{\eta}_1}{2\pi}\right]+\frac{2\nu_1}{\alpha}\frac{\partial\phi}{\partial z}, \tag{3a}$$

$$\eta_0 = \sum_{n=1}^{N}\mathrm{e}^{\epsilon n\eta}\left(A_n\exp\left[-\int_0^t\delta_n\,\mathrm{d}t\right]\cos n\xi-B_n\exp\left[-\int_0^t\beta_n\,\mathrm{d}t\right]\sin n\xi\right)-\frac{\bar{\eta}_0}{2\pi}. \tag{3b}$$

The constants $\bar{\eta}_0$ and $\bar{\eta}_1$ are found from the condition

$$\int_0^{2\pi} \eta_0 \, d\xi = 0, \quad \int_0^{2\pi} \eta \, d\xi = 0. \tag{3c}$$

The integral (3a) reduces by a factor of two the number of unknowns, thus making it much easier to obtain equations for the potential harmonics, as well as to find higher approximations and apply numerical methods.

To obtain equations for $A_i, B_i \, (i \geqslant 2)$, as well as for the phase velocity α and the damping δ_1, we shall insert the integral (3a) into the dynamical boundary condition (1b). Disregarding the terms of order δ_1^2 and $\delta_1 \epsilon$ and denoting the insignificant terms, related to ϕ_0 and $\bar{\eta}_{0,1}$, through $\tilde{\phi}_0$ we find

$$\begin{aligned}
\sum_{n=1}^{N} e^{\epsilon n \eta} \Bigg\{ \cos n\xi \Bigg[A_n \exp\Bigg[-\int_0^t \delta_n \, dt \Bigg] (1 - \alpha n + T n^2) + B_n \exp\Bigg[-\int_0^t \beta_n \, dt \Bigg] \\
\times \left(\alpha + \frac{1}{n} + Tn \right) \left(\frac{2\nu_1 n^2}{\alpha} - \beta_n \right) \Bigg] + \sin n\xi \Bigg[-B_n \exp\Bigg[-\int_0^t \beta_n \, dt \Bigg] (1 - \alpha n + T n^2) \\
+ A_n \exp\Bigg[-\int_0^t \delta_n \, dt \Bigg] \left(\alpha + \frac{1}{n} + Tn \right) \left(\frac{2\nu_1 n^2}{\alpha} - \delta_n \right) \Bigg] \Bigg\} \\
+ \tfrac{1}{2} \epsilon \alpha (\nabla \phi)^2 - T \left[\frac{\eta_{\xi\xi}}{(1 + \epsilon^2 \eta_\xi^2)^{\frac{3}{2}}} + \Delta \right] = \tilde{\phi}_0.
\end{aligned} \tag{4}$$

Here the last two terms on the left-hand side are proportional to ϵ to a power not less than unity; Δ is equal to the sum of terms taking into account the influence of surface tension in the first term.

Multiplying (4) by $\cos n\xi$ or $\sin n\xi$ and integrating over the wave period we can obtain differential equations for the potential harmonic amplitudes A_n and B_n. However, it is rather time consuming to consider a large number of such equations even with the aid of modern computers.

The problem is simplified for quasi-stationary waves whose amplitudes change rather slowly. The quantities δ_n and β_n for $n > 1$ in (4) can be considered equal to zero till the variation rate of higher resonance harmonics excited by lower ones is less than their intrinsic damping rate, i.e. $\delta_n, \beta_n \ll 2\nu_1 n^2/\alpha$ since for non-resonance harmonics the neglect of δ_n and β_n is valid owing to the large mismatch $[1 - \alpha n + Tn^2]$. In such an approximation, higher harmonics are defined through the first one (at given phase velocity α and damping δ_1) by nonlinear algebraic equations. After solving these equations at $t = 0$ we can determine α and δ_1 as a function of ϵ from the equation for the first harmonic amplitude bearing in mind that $A_1 = 1, B_1 = 0$. In other words, defining α and δ_1 reduces the problem to finding the eigenvalues of the set of nonlinear equations.

Within the framework of such an approach we can roughly take into account the influence of non-stationary CGR generation by assuming that δ_n and β_n are expressed through δ_1 by

$$\delta_n = \delta_1 \frac{\epsilon}{A_n} \frac{\partial A_n}{\partial \epsilon}, \quad \beta_n = \delta_1 \frac{\epsilon}{B_n} \frac{\partial B_n}{\partial \epsilon}. \tag{5}$$

This approximation can be called the second-order quasi-stationary approximation. For space-periodic waves, such a definition clearly does not lead to fundamental effects and we shall not focus on it. However, when the propagation of quasi-periodic

GCW is analysed, an analogous definition could be necessary to investigate the GCW self-modulation processes, for example.

As the calculations showed, with large steepness of GCW the conditions of quasi-stationarity for resonance harmonics become less applicable. For example, with $\Lambda = 5$ cm for the limiting steepness $2A/\Lambda = 0.058$ (where A is GCW amplitude), for which results are obtained by the proposed method, and for the number of the resonance harmonic $n = 10$, $\delta_n \alpha/2\nu_1 n^2 \approx 0.2$. With further increase of GCW steepness this ratio increases more. Nevertheless, the wave form, phase velocity and damping δ^*, specified above, have a definite physical meaning in this case as well. Indeed, assuming that the wind influence can be taken into account by introducing the increment γ_ω for the first harmonic of the potential we find that with viscosity taken into account there can exist a nonlinear stationary solution determined by the same equation for A_n, B_n as the quasi-stationary one at $\delta^* = \gamma_\omega$.

To define the quasi-stationary GCW characteristics we write a nonlinear system which follows from (4) in such a form that along with the unknowns $A_i, B_i\,(i \geqslant 2)$ there are also α and δ_1:

$$\left.\begin{aligned} M_{m,1}\alpha + M_{m,n}A_n + N_{m,1}\delta_1 + N_{m,n}B_n &= F_m, \\ L_{m,1}\alpha + L_{m,n}A_n + K_{m,1}\delta_1 + K_{m,n}B_n &= \mathscr{F}_m. \end{aligned}\right\} \tag{6}$$

In system (6) the summation is over repeated indices; $m = (1,\ldots,N), n = (2,\ldots,N)$; the coefficients and the right-hand sides are functions of the potential harmonic amplitude, the damping coefficient and the phase velocity α. They have the form

$$M_{m,1} = -AC_{m,1}(1-\epsilon^2), \tag{7}$$

$$M_{m,2} = AC_{m,2}\left[-2\alpha + 1 - 4T + \epsilon^2(-12T+3\alpha) + BC_{m,2}\left[2\nu_1\left(4+\frac{2}{\alpha}+8\frac{T}{\alpha}\right) - \delta_2(\tfrac{1}{2}+\alpha+2T)\right]\right] + \gamma_{m,2}, \tag{8}$$

$$\gamma_{m,2} = 2\epsilon[AC_{m,1}(\alpha - \tfrac{3}{2}T) + AC_{m,3}\tfrac{9}{2}T + 12(A_2 AC_{m,4} - B_2 BC_{m,4})] + \epsilon^2 15TAC_{m,4}, \tag{9}$$

$$M_{m,n} = AC_{m,n}[-\alpha n + 1 + Tn^2] + BC_{m,n}\left(\frac{1}{n}+\alpha+Tn\right)(2\nu_1 n^2/\alpha - \delta_n) + \gamma_{m,n}, \tag{10}$$

$$\begin{aligned}\gamma_{m,n} = {} & \epsilon n[AC_{m,n-1}(\alpha - \tfrac{1}{2}T(n+1)) + AC_{m,n+1}\tfrac{3}{2}T(n+1) + (2\alpha - T(n+2))(A_2 AC_{m,n-2} \\ & + B_2 BC_{m,n-2}) + 3T(n+2)(A_2 AC_{m,n+2} - B_2 BC_{m,n-2})] - \tfrac{1}{8}\epsilon^2 Tn[LAC_{m,n-2}(n+6) \\ & - 15AC_{m,n+2}(n+2)] + \epsilon^2 nAC_{m,n-2}(\alpha + T(n+1)),\end{aligned} \tag{11}$$

$$F_m = R_m + \tilde{\gamma}_{m,1} + \tilde{\gamma}_{m,n}A_n + \tilde{\zeta}_{m,n}, \tag{12}$$

$$\tilde{\gamma}_{m,1} = AC_{m,1}(\epsilon^2\alpha - 1) - BC_{m,1}4\nu_1, \tag{13}$$

$$\tilde{\gamma}_{m,n} = T\left[AC_{m,n}n^2 + BC_{m,n}\left(\frac{2\nu_1 n^3}{\alpha} - \delta_n n\right)\right] + \gamma_{m,n}. \tag{14}$$

Here

$$AC_{m,n} = \int_{-\pi}^{\pi} e^{\epsilon n\eta}\cos nx\cos mx\,dx; \quad BC_{m,n} = \int_{-\pi}^{\pi} e^{\epsilon n\eta}\sin nx\cos mx\,dx;$$

$$R_m = \int_{-\pi}^{\pi}\{T\eta_{xx}/[1+(\epsilon\eta_x)^2]^{\frac{3}{2}} - \tfrac{1}{2}\epsilon\alpha(\nabla\phi)^2\}\cos mx\,dx$$

is the Fourier cosine coefficients of these functions. L in (11) is equal to unity. The coefficients $N_{m,n}, \tilde{\zeta}_{m,n}$ are obtained from relations (8)–(11) and (14) for $M_{m,n}, \tilde{\gamma}_{m,n}$ by substitutions $\delta_n \to \beta_n$, $AC_{m,n} \to -BC_{m,n}$, $BC_{m,n} \to AC_{m,n}$ and in (11) one should put $L = -1$, while

$$N_{m,1} = -BC_{m,1}(1+\alpha+T). \tag{15}$$

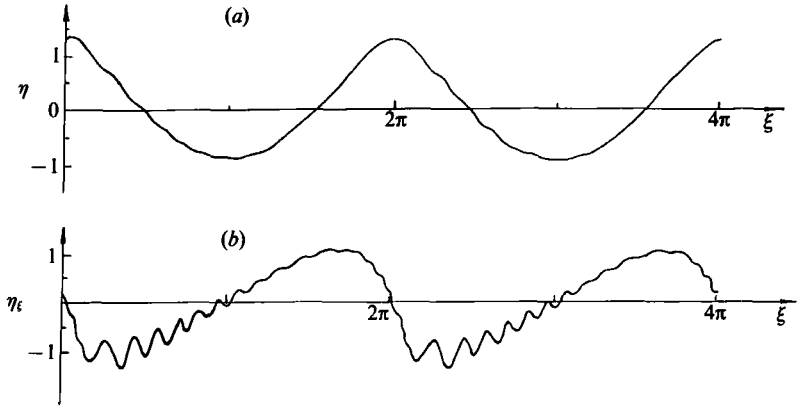

FIGURE 1. (*a*) The form of the free surface of GCW and (*b*) its first derivative, at $\Lambda = 6$ cm, $2A/\Lambda = 0.066$.

The quantities $L_{m,1}, L_{m,n}$ are obtained from (7)–(11) by the substitutions

$$AC_{m,n} \to AS_{m,n} = \int_{-\pi}^{\pi} e^{\epsilon n\eta} \cos nx \sin mx \, dx, \quad BC_{m,n} \to BS_{m,n}$$
$$= \int_{-\pi}^{\pi} e^{\epsilon n\eta} \sin nx \sin mx \, dx$$

at $L = 1$ in (11). In order to find $K_{m,n}$, the substitutions $AC_{m,n} \to -BS_{m,n}$, $BC_{m,n} \to AS_{m,n}$, $\beta_n \to \delta_n$ are needed, and with $L = -1$ in (11). The right-hand side of (6), $\mathscr{F}_m$, is sought from relations (12)–(14) if

$$R_m \to T_m = \int_{-\pi}^{\pi} [T\eta_{xx}/[1+(\epsilon\eta_x)^2]^{\frac{3}{2}} - \tfrac{1}{2}\epsilon\alpha(\nabla\phi)^2] \sin mx \, dx$$

and substitutions $AC_{m,n} \to AS_{m,n}$, $BC_{m,n} \to BS_{m,n}$ are made in $\tilde{\gamma}$ and $\tilde{\zeta}$.

The coefficients on the left-hand side of (6) consist (see (7)–(11)) of a part independent of ϵ (for the harmonic amplitude coefficients this corresponds to dispersion equations with damping taken into account) and a part dependent on ϵ in the first and second power. The second part consists of quadratic and cubic terms (that correspond to self-modulation, cross-modulation and parametric interaction) taken from the last two terms on the left-hand side of (4). The remainder of these terms is on the right-hand side of (6). This partition is to ensure that the determinant of (6) does not become zero because of the higher-harmonic resonance when the above method of solution is used.

Equation (6) together with (3) was solved with a computer by the iteration method. As initial condition we put $A_1 = 1, B_1 = 0, A_i, B_i = 0 (i > 1)$; the initial values of α and δ_1 were approximated by the values following from the weakly nonlinear theory, δ_n and β_n at $n > 1$ were considered equal to zero ($\beta_1 \equiv 0$). Then from (3) we found the form of the surface η by iteration. Thereafter we determined the right-hand sides and the coefficients in (6) and then calculated new values of A_i, B_i, α and δ_1. The cycle was repeated till the relative error in defining the sought values became smaller than a given error (this error was 1% for harmonics with $C_n = (A_n^2 + B_n^2)^{\frac{1}{2}} \geqslant 10^{-6}$ and $\log C_n$% at $C_n < 10^{-6}$).

The wave form obtained the manner given above (figure 1) is in good agreement with the experimental data of Ermakov *et al.* (1986). Using the GCW profiles we can

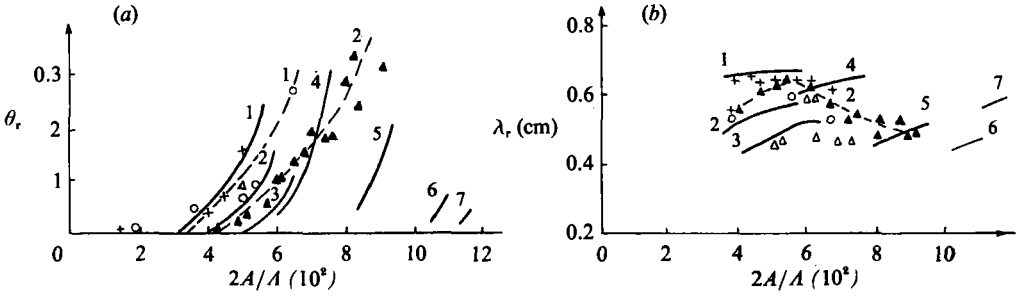

FIGURE 2. The dependence of (*a*) the ripple steepness and (*b*) its wavelength at the crest of GCW on their steepness. Solid curves correspond to theoretical results (curves 1–3 are obtained by the improved first Stokes method; curves 4–7 are obtained by the multiple-scale method): curve 1, $\Lambda = 4$ cm; 2, $\Lambda = 5$ cm; 3, $\Lambda = 6$ cm; 4, $\Lambda = 7$ cm; 5, $\Lambda = 10$ cm; 6, $\Lambda = 15$ cm; 7, $\Lambda = 20$ cm. Dashed curves correspond to averaged experimental results: curve 1, $f = 5.9$ Hz ($\Lambda_0 = 5$ cm); 2, $f = 4$ Hz ($\Lambda_0 = 10$ cm). Λ_0 is the wavelength of GCW in the linear approximation. Experimental points correspond to the following GCW frequencies: +, $f = 7$ Hz ($\Lambda_0 = 3.9$ cm); ○, $f = 5.9$ Hz ($\Lambda_0 = 5$ cm); △, $f = 4.8$ Hz ($\Lambda_0 = 7$ cm); ▲, $f = 4$ Hz ($\Lambda_0 = 10$ cm).

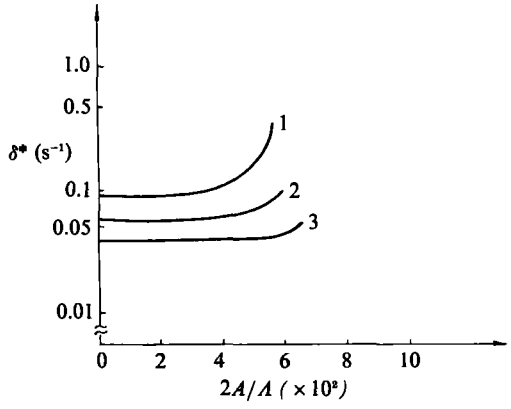

FIGURE 3. Dependence of the nonlinear decrement of GCW due to ripple generation on their steepness: curve 1, $\Lambda = 4$ cm; 2, $\Lambda = 5$ cm; 3, $\Lambda = 6$ cm.

find the dependence of ripple steepness (curves 1–3 in figure 2*a*) and wavelength (curves 1–3 in figure 2*b*) at the crests of GCW on the GCW steepness $2A/\Lambda$, where A is the wave amplitude. From these figures it is seen that, as in the experiment, the ripple steepness at the crests grows rapidly with increasing steepness of GCW while the ripple wavelength remains practically unchanged. Figure 3 shows the dependence of the damping δ_1 on the steepness of GCW at several values of the wavelength of the GCW. In this case, the decrease of GCW increases sharply in the parameter range where CGR are excited intensely, as was to be expected. This is another proof of the conclusion of Longuet-Higgins (1963), Ruvinsky & Freidman (1981), and Ermakov *et al.* (1986) that the ripple excitation damps the GCW.

Because of the limited volume of operative memory, the computer we used (64 kB) permitted us to take into account only 27 harmonics of the GCW potential. This determined the wavelength (4–6 cm) and the steepness range of these waves (see figure 2*a*) for which correct results could be achieved by such a method. At large wavelength and steepness of GCW the second harmonic of CGR began to be excited intensely in the displacement spectrum. This stimulated resonance corresponds to

higher harmonics than those taken account of in the potential and distorts significantly the wave profile. Hence, to describe correctly the second harmonic of the ripple, a corresponding number of harmonics (more than we could achieve) must be retained in the potential, i.e. more powerful computers are required.

It should also be borne in mind that this method is inapplicable when a strongly nonlinear CGR is excited and the displacement becomes an unambiguous function of the horizontal coordinate. When studying such 'superstrong' GCW it is necessary to consider as independent variables quantities, the displacement dependence on which is ambiguous, e.g. the potential and the current function, like when the second Stokes method is used (Stokes 1880; Chen & Saffman 1979, 1980). The wave surface deviation from the current line ($\Psi = \text{const}$) can approximately be defined from relations (3) bearing in mind that in the zero approximation (with respect to the amplitude variation velocity) the function $\eta_0(t, \phi)$ in (3.1) is governed by the equation $\Psi = \Psi_0$. Evidently, 'superstrong' quasi-stationary GCW do not form in nature because of the fast increase of the nonlinear damping of GCW with increasing amplitude of CGR excited on the crests of the GCW. Therefore, the investigation of such waves is still an unsolved problem of fundamental interest.

3. Extension to higher wavelengths: the multiple-scale method

In some cases, for example at the upper boundary of the GCW wavelength range, where the necessity of taking into account a large number of harmonics can lead to insurmountable computational difficulties with a 'straightforward' solution of the problem, it should be reasonable to consider separately a large-scale and a small-scale motion.

Let us represent the potential and the displacement as $\phi_1 = \phi^* + \phi_r$ and $\eta_1 = \eta^* + \eta_r$, where ϕ^* and η^* determine the large-scale motion (GCW part), while ϕ_r and η_r describe the small-scale motion (ripples). To obtain for the GCW part, we shall make use of the spectral method proposed. The velocity α and N_0 potential harmonics that define GCW, as well as the decrement δ_1 are found from the $2N_0$ equations obtained from (4) by corresponding Fourier transforms.

Assuming that the ripple steepness is small we can determine the ripple characteristics by obtaining from (1), analogously to Ruvinsky & Freidman (1981), a linear boundary-value problem with variable coefficients and driving force:

$$\nabla^2 \phi_r = 0, \tag{16a}$$

$$\frac{\partial \phi_r}{\partial t_1} - U_0(s, t_1)\frac{\partial \phi_r}{\partial s} + g(s, t_1)\,\eta_r - \gamma \frac{\partial^2 \eta_r}{\partial s^2} + 2\nu \frac{\partial^2 \phi_r}{\partial n^2} = \mathscr{F}(s, t_1)\Big|_{n=0}, \tag{16b}$$

$$\left(\frac{\partial}{\partial t_1} - U_0(s, t_1)\frac{\partial}{\partial s}\right)\left(\frac{\partial \eta_r}{\partial t_1} - U_0 \frac{\partial \eta_r}{\partial s} - \frac{\partial \phi_r}{\partial n} - \eta_r \frac{\partial U_0}{\partial s}\right) = 2\nu \frac{\partial^3 \phi_r}{\partial n\, \partial s^2}\Big|_{n=0}. \tag{16c}$$

$$\frac{\partial \phi_r}{\partial n} \to 0 \quad \text{at} \quad n \to -\infty. \tag{16d}$$

Here s and n are the respective coordinates along the steep wave surface and along the external normal to it; $U_0(s, t_1) = \partial \phi^*/\partial s$, the fluid velocity in GCW along the free surface; $g(s, t_1)$, the normal component of gravitational acceleration.

Without specifying the driving force $\mathscr{F}(s, t_1)$ we find the solution of set (16) in the WKB (geometrical optics) approximation. In the reference frame related to GCW we

should find stationary small-scale corrections to the steep wave. We therefore seek a solution in the form

$$\phi_r = \Phi \exp\left[\mathrm{i}\int_{s_0}^{s} k_r(s)\,\mathrm{d}s + \int_0^n \kappa_r(n)\,\mathrm{d}n\right] + \text{c.c.}, \quad \eta_r = H\exp\left[\mathrm{i}\int_{s_0}^{s} k_r(s)\,\mathrm{d}s\right] + \text{c.c.}$$

Expressing the potential amplitude through the displacement amplitude from (16*c*) and substituting the result into (16*b*) we obtain an inhomogeneous differential equation for H. Using the methods of variable differentiation and arbitrary constant variation we find that the ripple steepness $\theta_r = 2Hk_r$ is given by

$$\theta_r = \frac{k_r \exp\left[-\int_{s_0}^{s} \frac{2\nu k_r^2}{V-U_0}\,\mathrm{d}s_1\right]}{(U_0(V-U_0))^{\frac{1}{2}}} \int_{s_0}^{s} \frac{\mathscr{F}(s_1)\cos\left(\int_{s_0}^{s_1} k_r(s_2)\,\mathrm{d}s_2\right)\exp\left[\int_{s_0}^{s_1} \frac{2\nu k_r^2\,\mathrm{d}s_2}{V-U_0}\right]}{(U_0(V-U_0))^{\frac{1}{2}}}\,\mathrm{d}s_1. \quad (17)$$

Here $U_0 = c-(\epsilon c/k)(\partial\phi/\partial s)$; ϕ is determined by (2) at $N = N_0$; the coordinate $s \approx x+O(\theta^2)$, where θ is the steepness of GCW; $V = \frac{1}{2}U_0+\gamma k_r/U_0$ is the group velocity of the ripple on quiescent fluid. The wavenumber k_r is found from the dispersion relation:

$$k_r = \left(\frac{U_0}{2\gamma}\right)^2 + \left[\left(\frac{U_0}{2\gamma}\right)^4 - k_0^2\right]^{\frac{1}{2}}, \quad k_0^2 = \frac{g}{\gamma}, \quad \kappa_r|_{n=0} = |k_r|.$$

To find the ripple steepness in (17), the driving force $\mathscr{F}(x)$ must be determined sequentially. Bearing in mind the method used in defining the large-scale motion we find that this force represents the difference between the left-hand side of (4), taken at $N = N_0$, and the sum of its N_0 harmonics. Numerical calculations show that the main contribution to the driving force is yielded, as was predicted by Longuet-Higgins (1963), Ruvinsky & Freidman (1981), and Ermakov *et al.* (1986), by the term related to surface tension, i.e. proportional to the curvature K. However, to define accurately the higher harmonics of this 'force', which we are interested in, it is necessary to take into account the finite number of non-resonant harmonics of the potential, for which the surface tension is essential.

The numerical simulation of small-scale ripple excitation indicates that the multiple-scale method yields results in qualitative agreement with the experimental data for sufficiently long GCW in the range $\Lambda \gtrsim 7$ cm. With increasing the number of the potential harmonics taken into account in the large-scale motion from 4–5 to several below the resonant harmonic, the ripple parameters (figure 4) change little, not more than 10–15% (because of these inaccuracies the dependence $\lambda_r(\Lambda)$ can be a non-monotonic one (figure 2*b*)). This is an indication that when describing a large-scale motion we can restrict ourselves to 4–5 harmonics of the potential.

Figure 4(*a*, *b*) shows the calculated changes in steepness $\theta_r(x)$ and wavelength $\lambda_r(x)$ along the GCW. This figure shows one trough-to-trough wave period. It is seen that the ripple is excited at the crest of the GCW and its wavenumber changes significantly in this region. Therefore, the finiteness of the source region and the inhomogeneity of the fluid velocity there must be taken into account. Because of this, the ripple parameters should be determined not at the top of the GCW but at the end of the excitation region (figure 4).

Figure 2 (curves 4–7) shows the dependence of θ_r and λ_r on the GCW steepness and wavelength, found by the multiple-scale method. The lower limit on this dependence $\theta_r(A/\Lambda)$ at a fixed Λ is determined by the difficulty in distinguishing small higher harmonics from large lower ones, in the numerical experiment. The upper limit depends on the approach to the group synchronism of ripples and GCW and on the

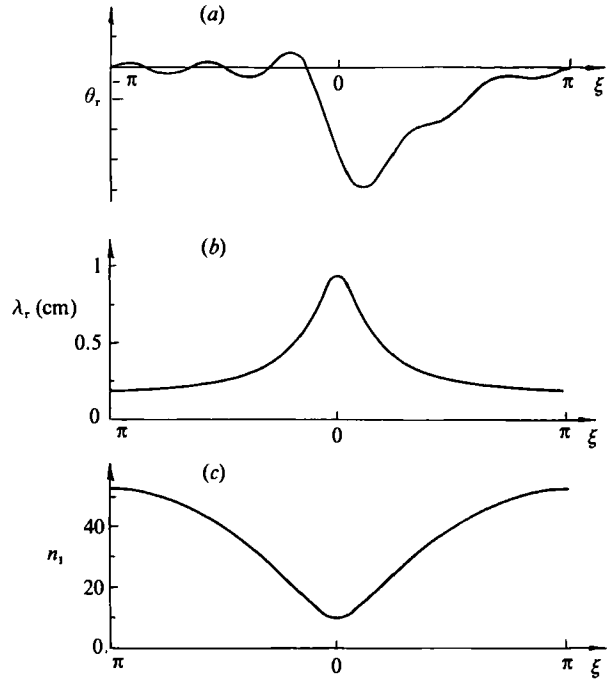

FIGURE 4. Dependence of (*a*) the ripple steepness, (*b*) wavelength and (*c*) dimensionless wavenumber $n_1 = k_r/k = \Lambda/\lambda_r$ on the dimensionless distance to the crest of GCW at the steepness $2A/\Lambda = 0.091$, the wavelength $\Lambda = 10$ cm and the number of potential harmonics that form GCW proper, $N_0 = 5$. When plotting the dependence $\theta_r(\xi)$ in (*a*) the harmonics beginning from the sixth are filtered.

applicability range of the WKB approximation, where this dependence is obtained. It is seen that the experimental and theoretical results are in qualitative agreement. However, bearing in mind the accuracy of the numerical and laboratory experiments, it should be apparent that the true ripple characteristics are between these two limits.

Taking into account the data of Longuet-Higgins (1978*a*, *b*) on the breaking of surface waves with steepness $2A/\Lambda$ greater than 0.13, the results we obtained (curve 7 in figure 2*a*) indicate that the long-wave limit of GCW capable of exciting ripples without breaking is a wavelength of the order of 20 cm.

4. Summary and conclusions

The theoretical investigation in this paper explains and describes quantitatively to a remarkable degree the phenomenon of CGR excitation by stationary and quasi-stationary GCW. It is therefore possible to obtain the ripple characteristics from the GCW characteristics, as well as the nonlinear damping of these waves related to the ripple excitation. An important problem is still unresolved concerning the upper limit (with respect to the GCW wavelength and steepness) on the applicability range of the improved first Stokes method. This requires the use of more powerful computers where one can take into account several hundreds of GCW harmonics.

These results can be used to estimate the surface-wave spectra in the centimetre and millimetre regions under natural conditions, although there the ripple excitation is non-stationary. This is confirmed by the fact recently ascertained by Ermakov, Ruvinsky & Salashin (1988) on the basis of the numerical calculations in the paper

and the experiments of Ermakov *et al.* (1988). Namely, it is found that the ripple characteristics are approximately determined by only one parameter – the radius of curvature of the GCW crest. It is therefore possible, knowing the distribution function of the surface curvature and the characteristics of ripples excited by an individual crest, to find the ripple spectrum. On the other hand, the relationship between the nonlinear damping of GCW and ripple excitation, which we obtained in this paper, permits one to investigate the spectrum evolution of GCW themselves (Ruvinsky & Freidman 1989) on the basis of the phenomenological kinetic equation proposed by Ruvinsky & Freidman (1985*b*). Using this equation one can also study the interaction of long surface waves with the GCW spectrum and its modulation by internal waves.

Thus, the results obtained in this paper can be used to solve a number of problems when the high-frequency region of the surface wave spectrum is investigated.

Appendix. Quasi-potential approximation for the description of nonlinear gravity-capillary waves on the surface of a viscous fluid

In this Appendix we give approximate equations, called below the quasi-potential equations, to simplify the investigation of the influence of viscosity on nonlinear surface waves.

For linear gravity–capillary waves (GCW) the quasi-potential approximation was proposed by Ruvinsky & Freidman (1981) to take into account the damping of ripples excited by steep gravity waves. A model taking into account the damping under the boundary conditions for the potential component of the nonlinear GCW motion was used by West (1982). However, the model proposed by West (1982) is not quite correct since the damping yielded by this model is half the correct value for linear GCW. A closed set of quasi-potential equations for nonlinear GCW was first formulated without a detailed derivation by Ruvinsky & Freidman (1985*a*, *b*, 1987).

In this appendix we give a sequential derivation of the kinematic and dynamic boundary conditions for the potential component of the flow, which approximately takes into account the influence of viscosity, as well as the equations for the normal (to the free surface) component of the vortex flow. Together with the Laplace equations these last equations form a closed set of nonlinear quasi-potential equations.

When deriving the quasi-potential equations we use the fact, well-known from the linear theory of GCW damping (Lamb 1932; Landau & Lifshitz 1959), that in the case of low viscosity, which will be considered below, the vibrational part of the vortex flow component is localized in a narrow (compared to the penetration depth of the potential component) layer of thickness δ near the free surface. A similar situation permitting one to take into account the influence of viscosity only under the boundary conditions for the potential part of the motion, also arises when investigating the flow excited by a body with dimensions $l \gg \delta$ vibrating in liquid (Landau & Lifshitz 1959) as well as when defining the influence of energy dissipation in the bottom boundary layer on wave reflection from the shore (Mahony & Pritchard 1980).

As is well known (Whitham 1974), the kinematic boundary condition can be written in an invariant form:

$$-\frac{\partial F}{\partial t_1} = (\boldsymbol{U}\nabla) F \equiv U_n |\nabla F|. \tag{A 1}$$

Here $F(\boldsymbol{q}, t_1) = 0$ determines the free surface; $\boldsymbol{q}$ is the spatial coordinate, $\boldsymbol{U}$ is the fluid velocity, U_n is the normal component to the free surface.

In the case of low viscosity it can be assumed that the vibrational part of the flow in a surface wave in the laboratory reference frame $\boldsymbol{U}_1 = \nabla\phi_1 + \boldsymbol{v}_1$ consists of a potential component $\nabla\phi_1$ and a small vortex part $\boldsymbol{v}_1$ excited by the potential component. (In a linear approximation $|\boldsymbol{v}_1|/|\nabla\phi_1| \sim k/m = (2\pi/\lambda)(2\nu/\omega)^{\frac{1}{2}}$, where $k^{-1} = \lambda/2\pi$ and $m \equiv \delta = (2\nu/\omega)^{\frac{1}{2}}$ are respectively the penetration depth of the potential and the vortex component of the liquid velocity; ω and λ are characteristic time and space scales of GCW, respectively. For water at $\lambda \gtrsim 0.5$ cm we have $k/m \sim 10^{-2}$). The equation for the normal velocity component v_{1n}, involved in (A 1), can be found, as is shown below, from the equation for vorticity, the source of which is defined by the boundary condition for the tangential (to the surface) stress tensor component and the continuity equation.

For plane motion, which we shall consider below, the equation for vorticity

$$\boldsymbol{\Omega} = \boldsymbol{y}^0\Omega = \boldsymbol{y}^0 \frac{1}{(g_n g_s)^{\frac{1}{2}}}\left(\frac{\partial}{\partial s}(v_{1n} g_n^{\frac{1}{2}}) - \frac{\partial}{\partial n}(v_{1s} g_s^{\frac{1}{2}})\right)$$

in a laboratory system has the form

$$\frac{\partial \boldsymbol{\Omega}}{\partial t_1} + (\boldsymbol{u}_1 \nabla)\,\boldsymbol{\Omega} = \nu\nabla^2\boldsymbol{\Omega}. \tag{A 2}$$

Here s is the coordinate along the GCW surface (where $n = 0$), n is the coordinate along the normal to this surface; the unit vector $\boldsymbol{y}^0 = [\boldsymbol{s}^0 \times \boldsymbol{n}^0]$. The Lyame coefficients of this coordinate system are equal (Longuet-Higgins 1953): $g_n = 1, g_s = (1 + nK)^2$, where $K(n, s)$ is the curvature of the coordinate lines.

The fast-varying nonlinear terms in the equations of motion, which are due to the vortex velocity component, proportional to the product of two small parameters (the ratio k/m and the wave steepness), and at $k/m \ll 1$ they clearly cannot lead to noticeable effects. Therefore, when finding the oscillating part of the vortical motion one can restrict oneself to the linear approximation (in particular, the curvature of the coordinate lines is neglected).

As is known from the linear theory of GCW damping (Lamb 1932; Landau & Lifshitz 1959) $v_{1n}/v_{1s} \sim k/m \sim \lambda^{-1}(\nu/\omega)^{\frac{1}{2}} \ll 1$. Therefore it can be assumed that in a linear approximation the vorticity $\Omega \approx -\partial v_{1s}/\partial n$. Then from (A 2) we obtain at the first order in the ratio k/m

$$\frac{\partial^2 v_{1s}}{\partial n\,\partial t_1} = \nu\frac{\partial^3 v_{1s}}{\partial n^3}. \tag{A 3}$$

The boundary condition for (A 3) is the condition for the tangential component of the stress tensor on the free surface, which at $v_{1n}/v_{1s} \ll 1$ has the form:

$$\frac{\partial v_{1s}}{\partial n} = -2\frac{\partial^2 \phi_1}{\partial n\,\partial s}\bigg|_{n=0}. \tag{A 4}$$

From (A 3) with the boundary condition (A 4), which in fact defines the surface source of vorticity, one can find the quantity v_{1s} and then define the normal component v_{1n} from the continuity equation:

$$\frac{\partial v_{1n}}{\partial n} + \frac{\partial v_{1s}}{\partial s} = 0. \tag{A 5}$$

The quantity v_{1n} entering (A 1) at the boundary can be determined from (A 3)–(A 5) without finding v_{1n} inside the fluid. Differentiating (A 3) with respect to

s, we substitute $\partial v_{1s}/\partial s$ from (A 5) into the left-hand side and integrate it twice with respect to n. Then substituting $\partial v_{1s}/\partial n$ from (A 4) to the right-hand side we find

$$\frac{\partial v_{1n}}{\partial t_1} = 2\nu \frac{\partial^3 \phi_1}{\partial n\, \partial s^2}\bigg|_{n=0}. \tag{A 6}$$

Generally speaking, the integration of (A 6) involves the terms $A(s)\,n + B(s)$, where $A(s)$ and $B(s)$ are some functions. The first term is equal to zero since (A 6) is taken on the free surface (where $n = 0$) and the second term is assumed equal to zero since we seek a vortex flow excited by a potential flow.

To obtain a closed set of quasi-potential equations the boundary conditions (A 1), (A 6) must be supplemented with the boundary condition for the normal (to the free surface) component of the stress tensor. Bearing in mind that $v_{1n}/(\partial\phi_1/\partial n) \sim k/m \ll 1$, this boundary condition can be written as

$$\frac{p}{\rho} = \frac{p_0}{\rho} - \gamma K + 2\nu \frac{\partial^2 \phi_1}{\partial n^2}. \tag{A 7}$$

Here p and p_0 are the pressures inside and outside the fluid, respectively; ρ is the fluid density; $\gamma = \alpha/\rho$, where α is the surface-tension coefficient.

In the case of pure potential motion, p is substituted into (A 7) from the Bernoulli integral and the resultant equation is used as the dynamic boundary condition. In a similar fashion, we integrate the Navier–Stokes equation, written in a laboratory reference frame, along the vertical coordinate z_1 from $-\infty$ to the free surface $\eta_1(x_1, t_1)$:

$$\frac{\partial \phi_1}{\partial t_1} + \tfrac{1}{2}(\boldsymbol{v}_1 + \boldsymbol{\nabla}\phi_1)^2 + \frac{p}{\rho} + g z_1\big|_{n=0} = -\int_{\eta_1-\delta}^{\eta_1} \left(\frac{\partial v_{1z_1}}{\partial t_1} - \nu \nabla^2 v_{1z_1}\right) \mathrm{d}z_1 + \int_{\eta_1-\delta}^{\eta_1} [(\boldsymbol{v} + \boldsymbol{\nabla}\phi_1) \times \boldsymbol{\Omega}]\, \mathrm{d}z_1. \tag{A 8}$$

Here z_1 is the distance in the vertical direction from the chosen reference level of potential energy to the free surface; the pressure p is defined by (A 7); the width of a viscous boundary layer $\delta \sim 1/m$. To close the set of quasi-potential equations entering (A 8), the vertical velocity component can be found from (A 3)–(A 5). Meanwhile, among the terms describing the influence of viscosity in (A 8) we need take into account in the first approximation with respect to the small parameter k/m only the term $2\nu\partial^2\phi_1/\partial n^2$ in the relation for p (see (A 7)). (In fact, $\nu\partial^2\phi_1/\partial n^2 \sim \nu\theta$ where θ is the steepness of GCW;

$$\int_{\eta_1-\delta}^{\eta_1} \frac{\partial v_{1z_1}}{\partial t_1}\mathrm{d}z_1 \sim \frac{\nu^2}{\delta}\theta; \quad \int_{\eta_1-\delta}^{\eta_1} [\boldsymbol{\nabla}\phi_1 \times \boldsymbol{\Omega}]\, \mathrm{d}\boldsymbol{z}_1 = \delta\theta^2;$$

$$\int_{\eta_1-\delta}^{\eta_1} [\boldsymbol{v}_1 \times \boldsymbol{\Omega}]\, \mathrm{d}\boldsymbol{z}_1 \sim \delta^2\theta^2; \quad \boldsymbol{v}\boldsymbol{\nabla}\phi_1 \sim \delta\theta^2; \quad \delta \sim \nu^{\frac{1}{2}}.)$$

In this approximation (bearing in mind also that, accurate to quadratic terms $\partial^2\phi_1/\partial n^2 = -\partial^2\phi_1/\partial s^2$), the relation (A 8) can be written as

$$\frac{\partial \phi_1}{\partial t_1} + \tfrac{1}{2}(\boldsymbol{\nabla}\phi_1)^2 - \gamma K + g z_1 - 2\nu \frac{\partial^2 \phi_1}{\partial s^2} = 0\bigg|_{n=0}. \tag{A 9}$$

The nonlinear terms in the amplitude of the oscillations in these equations lead,

besides the fast-varying components, to a slowly varying vortical velocity U_v component. This is due to the transfer of the momentum of the damped wave motion to the vortex flow, the energy of which decreases continuously while the momentum is conserved (before the interaction with the walls). The velocity of this flow depends on the pre-history, the fluid volume configuration, the characteristics of the fluid volume boundaries (the walls and the bottom) (Dore 1985; Craik 1982). The velocity U_v need not be so small. For example, it can be easily shown using the momentum conservation law that when a spatially homogeneous wave with the initial vibrational velocity v_0 is damped, then a flow is excited whose velocity ($\Delta^2 U \approx v_0^2/c$) after the wave damping for strong waves ($v_0 \sim c$) can be close to their phase velocity c. In this case, the flow appears to be localized in a layer of depth $h_0 \sim k^{-1}$, which thereafter expands ($h \sim (\nu t)^{\frac{1}{2}}$).

The existence of a shear flow with a velocity discontinuity in the localization region of potential wave motion of the order of the phase velocity can, as is well known (see e.g. Lin 1955), lead to fundamental effects because of the coincidence layer. The above estimates show, however, that this is valid only for waves of nearly limiting steepness since $v_0 \sim c$ only for such waves. In the parameter range of interest $v_0 \ll c$ (figure 2) so that although U_v can be comparable with the phase velocity of the wave due to continuous accumulation, the velocity discontinuity at depth k^{-1} is of the order of ΔU, i.e. much less than c. Therefore, when determining the wave form and the wave parameters the shear flow can be either disregarded or assumed to be a given depth-homogeneous flow.

Thus the Laplace equation with boundary conditions (A 1), (A 6), (A 9) forms a closed set of quasi-potential invariant equations, which takes into account in the first approximation the influence of viscosity on the form and amplitude of GCW. If we define the free surface by the equation $F = z_1 - \eta_1(x_1, t_1)$, where x_1, z_1 are the Cartesian coordinates and bear in mind that $v_{1n} = v_{1z_1}$, $\partial^2\phi_1/\partial n^2 = \partial^2\phi_1/\partial z_1^2$; $\partial^3\phi_1/\partial n\,\partial s^2 = \partial^3\phi_1/\partial z_1\,\partial x_1$, in the linear approximation, then this set can be written as (1).

To investigate the structure and propagation of GCW with dissipation taken into account it is possible to use a simpler set than (1), permitting the model to take into account the influence of viscosity. This set follows from (1) if we put $v_{1z} = 0$ and substitute the coefficient (2ν) for (4ν) in the dynamic boundary condition. The use of such model boundary conditions is justified by the coincidence of the exactly found linear wave damping and the value obtained from this model set.

REFERENCES

Chang, J. H., Wagner, R. N. & Henry, C. V. 1978 Measurements of high frequency capillary waves on steep waves. *J. Fluid Mech.* **83**, 401–415.

Chen, B. & Saffman, P. G. 1979 Steady gravity–capillary waves on deep water. I. Weakly nonlinear waves. *Stud. Appl. Maths* **60**, 183–210.

Chen, B. & Saffman, P. G. 1980 Steady gravity–capillary waves on deep water. II. Numerical results for finite amplitude. *Stud. Appl. Maths* **62**, 95–111.

Craik, A. D. D. 1982 The drift velocity of water waves. *J. Fluid Mech.* **116**, 187–206.

Crapper, G. D. 1970 Non-linear capillary waves generated by steep gravity waves. *J. Fluid Mech.* **40**, 149–159.

Davis, T. V. 1951 The theory of symmetrical gravity waves of finite amplitude. I. *Proc. R. Soc. Lond.* A **208**, 475–486.

Dore, B. D. 1985 On wave-induced surface drift. *Wave Motion* **7**, 123–128.

Ermakov, S. A., Ruvinsky, K. D. & Salashin, S. G. 1988 Local relation between ripples on gravity–capillary wave crests and their curvature. *Izv. Atmos. Ocean. Phys.* **24**, 561–563.

ERMAKOV, S. A., RUVINSKY, K. D., SALASHIN, S. G. & FREIDMAN, G. I. 1986 Experimental investigation of capillary–gravity ripple generation by strongly nonlinear waves on the deep fluid surface. *Izv. Atmos. Ocean. Phys.* **22**, 835–842.

HOGAN, S. J. 1980 Some effects of surface tension on steep water waves. Part 2. *J. Fluid Mech.* **96**, 417–445.

HOGAN, S. J. 1981 Some effects of surface tension on steep water waves. Part 3. *J. Fluid Mech.* **110**, 381–410.

LAMB, H. 1932 *Hydrodynamics*, §349. Cambridge University Press.

LANDAU, L. D. & LIFSHITZ, E. M. 1959 *Fluid Mechanics*, §§24, 25. Pergamon.

LIN, C. C. 1955 *The theory of Hydrodynamic Stability*. Cambridge University Press.

LONGUETT-HIGGINS, M. S. 1953 Mass transport in water waves. *Phil. Trans. R. Soc. Lond.* A **245**, 535–581.

LONGUET-HIGGINS, M. S. 1963 The generation of capillary waves by steep gravity waves. *J. Fluid Mech.* **16**, 138–159.

LONGUET-HIGGINS, M. S. 1978*a* The instability of gravity waves of finite amplitude in deep water. I Superharmonics. *Proc. R. Soc. Lond.* A **360**, 471–488.

LONGUET-HIGGINS, M. S. 1978*b* The instability of gravity waves of finite amplitude in deep water. II Subharmonics. *Proc. R. Soc. Lond.* A **360**, 489–505.

MAHONY, J. J. & PRITCHARD, W. G. 1980 Wave reflection from beaches. *J. Fluid Mech.* **101**, 808–832.

ROTTMAN, J. W. & OLFE, D. B. 1979 Numerical calculation of steady gravity capillary waves using an integro-differential formulation. *J. Fluid Mech.* **94**, 777–793.

RUVINSKY, K. D. & FREIDMAN, G. I. 1981 The generation of capillary–gravity waves by steep gravity waves. *Izv. Atmos. Ocean. Phys.* **17**, 548–553.

RUVINSKY, K. D. & FREIDMAN, G. I. 1985*a* Improvement of the first Stokes method for the investigation of finite-amplitude potential gravity–capillary waves. In *IX All-Union Symp. on Diffraction and Propagation Waves. Theses of Reports*. Tbilisi, Vol. 2, pp. 22–25.

RUVINSKY, K. D. & FREIDMAN, G. I. 1985*b* Ripple generation on the gravity–capillary wave crests and its influence on the wave propagation. *Preprint* 132. Inst. Appl. Phys., Acad. Sci. USSR, Gorky. 46 pp.

RUVINSKY, K. D. & FREIDMAN, G. I. 1987 The fine structure of strong gravity–capillary waves. In *Nonlinear Waves: Structures and Bifurcations* (ed. A. V. Gaponov-Grekhov & M. I. Rabinovich), pp. 304–326. Moscow: Nauka.

RUVINSKY, K. D. & FREIDMAN, G. I. 1989 Phenomenological taking into account of nonlinear damping of gravity–capillary waves in the framework of the kinetic equation. *Izv. Atmos. Ocean. Phys.* **25**, 636–640.

SAFFMAN, P. G. & YUEN, H. C. 1985 Three-dimensional waves on deep water. In *Advances in Nonlinear Waves*, Vol. 2 (ed. L. Debnath), pp. 1–30. Pitman.

SCHWARTZ, L. W. & VANDEN-BROECK, J. M. 1979 Numerical solution of the exact equations for capillary-gravity waves. *J. Fluid Mech.* **95**, 119–139.

STOKES, G. G. 1880 Supplement to a paper on the theory of oscillatory waves. *Mathematical and Physical Papers*, Vol. 1, pp. 197–229. Cambridge University Press.

WEST, B. J. 1982 Statistical properties of water waves. Part 1. Steady-state distribution of wind-driven gravity–capillary waves. *J. Fluid Mech.* **117**, 187–210.

WHITHAM, G. B. 1974 *Linear and Nonlinear Waves*, §13.1. Wiley Interscience.

ZHANG, J. & MELVILLE, W. K. 1987 Three-dimensional instabilities of nonlinear gravity–capillary waves. *J. Fluid Mech.* **174**, 187–208.